



# Sequential Time-Kill, a Simple Experimental Trick To Discriminate between Pharmacokinetics/Pharmacodynamics Models with Distinct Heterogeneous Subpopulations versus Homogenous Population with Adaptive Resistance

A. Chauzy,<sup>a</sup> H. Ih,<sup>a,c</sup> M. Jacobs,<sup>a\*</sup>  S. Marchand,<sup>a,b</sup> N. Grégoire,<sup>a,b</sup>  W. Couet,<sup>a,b</sup>  J. M. Buyck<sup>a</sup>

<sup>a</sup>INSERM U1070 Pharmacologie des Anti-Infectieux, UFR de Médecine Pharmacie, Université de Poitiers, Poitiers, France

<sup>b</sup>Laboratoire de Toxicologie-Pharmacocinétique, CHU de Poitiers, Poitiers, France

<sup>c</sup>Pharmacy Department, Faculty of Medicine, Universitas Tanjungpura, Pontianak, Indonesia

A. Chauzy and H. Ih contributed equally to this work and are listed in alphabetical order.

**ABSTRACT** Experiments were conducted with polymyxin B and two *Klebsiella pneumoniae* isogenic strains (the wild type, KP\_WT, and its transconjugant carrying the mobile colistin resistance gene, KP\_MCR-1) to demonstrate that conducting two consecutive time-kill experiments (sequential TK) represents a simple approach to discriminate between pharmacokinetics/pharmacodynamics models with two heterogeneous subpopulations or adaptive resistance.

**KEYWORDS** *Klebsiella pneumoniae*, PK/PD model, antibiotic resistance, pharmacodynamics, polymyxin B, sequential time-kill

Semimechanistic pharmacokinetics/pharmacodynamics (PK/PD) modeling is a modern approach that offers unique opportunities to simulate CFU versus time after antibiotic exposures corresponding to various multiple-dosing strategies (1). Time-kill (TK) experiments constitute a simple and inexpensive approach to generate *in vitro* data in static conditions for antibiotics PK/PD modeling. After an initial decay of CFU with time, regrowth is frequently observed that can be described by a number of models. However, in the absence of precise mechanistic information, PD models with two stable, heterogeneous subpopulations, i.e., sensitive (S) and resistant (R) (referred to as S/R), would most often demonstrate superiority over models relying on adaptation phenomena (2). Although these models should then be challenged in dynamic (hollow-fiber) conditions, these experimental settings are much more expensive and complex to handle than TK experiments. However, conducting two consecutive TK experiments (sequential TK) may offer a pragmatic alternative. Indeed, the S/R model assumes that initial decay is due to the (S) disappearance and regrowth to (R) selection. However, the (S) and (R) subpopulations are supposed to be stable with time, so no regrowth would be expected after conducting a second TK experiment with the resistant subpopulation bacteria that regrew after the first TK experiment. Such a second regrowth would rather suggest progressive adaptation. Our objective was to confirm experimentally that sequential TK would offer a simple approach to discriminate between regrowth due to heterogeneous subpopulations and adaptive resistance (AR).

Two isogenic isolates were used in this study: a wild-type *Klebsiella pneumoniae* R2292 (KP\_WT) and its transconjugant carrying the mobile colistin resistance gene MCR-1 (KP\_MCR-1), kindly provided by P. Nordmann (University of Fribourg, Switzerland). This strain was built by transferring the MCR-1 plasmid from MCR-1-positive *Escherichia coli* isolates as donors (3). TK experiments were conducted in duplicate in

**Citation** Chauzy A, Ih H, Jacobs M, Marchand S, Grégoire N, Couet W, Buyck JM. 2020. Sequential time-kill, a simple experimental trick to discriminate between pharmacokinetics/pharmacodynamics models with distinct heterogeneous subpopulations versus homogenous population with adaptive resistance. *Antimicrob Agents Chemother* 64:e00788-20. <https://doi.org/10.1128/AAC.00788-20>.

**Copyright** © 2020 American Society for Microbiology. All Rights Reserved.

Address correspondence to W. Couet, [william.couet@univ-poitiers.fr](mailto:william.couet@univ-poitiers.fr).

\* Present address: M. Jacobs, Technologie Servier, Vignat Orleans, France.

**Received** 23 April 2020

**Returned for modification** 26 May 2020

**Accepted** 5 June 2020

**Accepted manuscript posted online** 8 June 2020

**Published** 22 July 2020

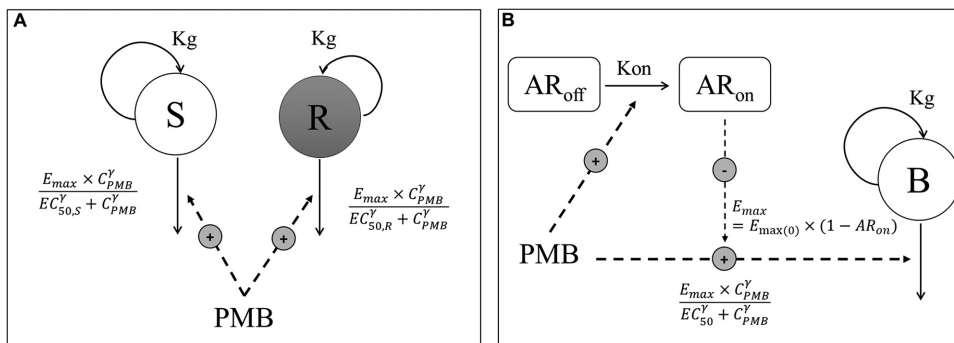


**FIG 1** Schematic illustrations of the S/R model (A) and AR model (B).  $C_{PMB}$ , PMB concentration; S, compartment with PMB-sensitive bacteria; R, compartment with resistant bacteria; B, compartment with homogenous bacterial population;  $K_g$ , rate constant for multiplication of bacteria;  $E_{max}$ , maximum kill rate constant;  $E_{max(0)}$ , maximum kill rate constant when no adaptive resistance has developed;  $EC_{50}$ , PMB concentration producing 50% of  $E_{max(0)}$ ;  $EC_{50,S}$  and  $EC_{50,R}$ , PMB concentration producing 50% of  $E_{max}$  for (S) and (R) bacteria, respectively;  $\gamma$ , sigmoidicity factor;  $AR_{off}$  and  $AR_{on}$ , compartments describing adaptive resistance being off and on, respectively;  $K_{on}$ , rate constant for development of adaptive resistance.

cation-adjusted Mueller-Hinton broth over 30 h at an initial inoculum close to  $10^6$  CFU/ml in the presence of polymyxin B (PMB) ranging from 0.0625 to 1 mg/liter for KP\_WT and 0.5 to 8 mg/liter for KP\_MCR-1. At 30 h, bacteria that regrew up to  $10^8$  CFU/ml were harvested by centrifugation and resuspended to immediately begin the second TK experiment at an initial inoculum close to  $10^6$  CFU/ml again, with PMB concentrations ranging from 0.0625 to 1 mg/liter for KP\_WT and 1 to 32 mg/liter for KP\_MCR-1. Modeling was conducted after the first TK and then simultaneously after the two sequential TK experiments for both strains, using NONMEM 7.4 with Laplacian numerical algorithm and the M3 method for handling observations below the limit of quantification (4). Each model incorporated a logistic growth expression to describe bacterial population dynamics. PMB bactericidal effect was modeled according to an  $E_{max}$  function for both strains. Two different model structures were investigated to characterize the emergence of resistance. The first model, S/R, includes two independent subpopulations of bacteria with different susceptibilities and regrowth explained by a higher  $EC_{50}$  (concentration that produces 50% of  $E_{max}$ ) value for the (R) than the (S) subpopulation (Fig. 1A) (5–7). The fraction of (S) and (R) bacteria in the initial inoculum was estimated as a parameter, and fitness cost resulting in a lower growth rate for the (R) subpopulation was investigated. The second model, AR, includes a single homogenous bacterial population with adaptive resistance (Fig. 1B). At the beginning of the experiment, all bacteria were assumed to be nonadapted, but an adaptation developed over time in the presence of PMB, affecting  $E_{max}$  (8). The fraction of (S) and (R) or adapted bacteria, depending on the model, at the end of the first TK experiment was used as the initial condition for the second TK experiment. Model selection was based on objective function value and goodness-of-fit plots. For nonnested models, the Bayesian information criterion (BIC) was calculated and compared between models.

Genes assumed to be involved in polymyxin resistance, i.e., *pmrA*, *pmrB*, *phoP*, *phoQ*, *pmrC*, *pmrE*, *lpxM*, *arnT*, *cptA*, *lpxT*, *eptB*, and *mcr-1*, were sequenced. Expression was analyzed by real-time quantitative PCR (RT-qPCR) and analyzed with the  $2^{-\Delta\Delta CT}$  method, by normalizing the relative expression of selected genes to the expression of *rpsL* used as an internal control (9), to determine their expression levels before and after the first and second TK experiments for both strains.

An initial CFU decay followed by regrowth was observed in both strains after the first single TK experiment, at PMB concentrations of 0.125 mg/liter for KP\_WT and 1.0 and 2.0 mg/liter for KP\_MCR-1 (Fig. 2). The S/R and AR models provided relatively good data fitting, although, as expected, statistical comparisons favored the S/R model (see BIC values in Table 1) (2). However, differences were observed between strains during the second TK experiment. In the presence of KP\_WT, PMB apparent activity was slightly

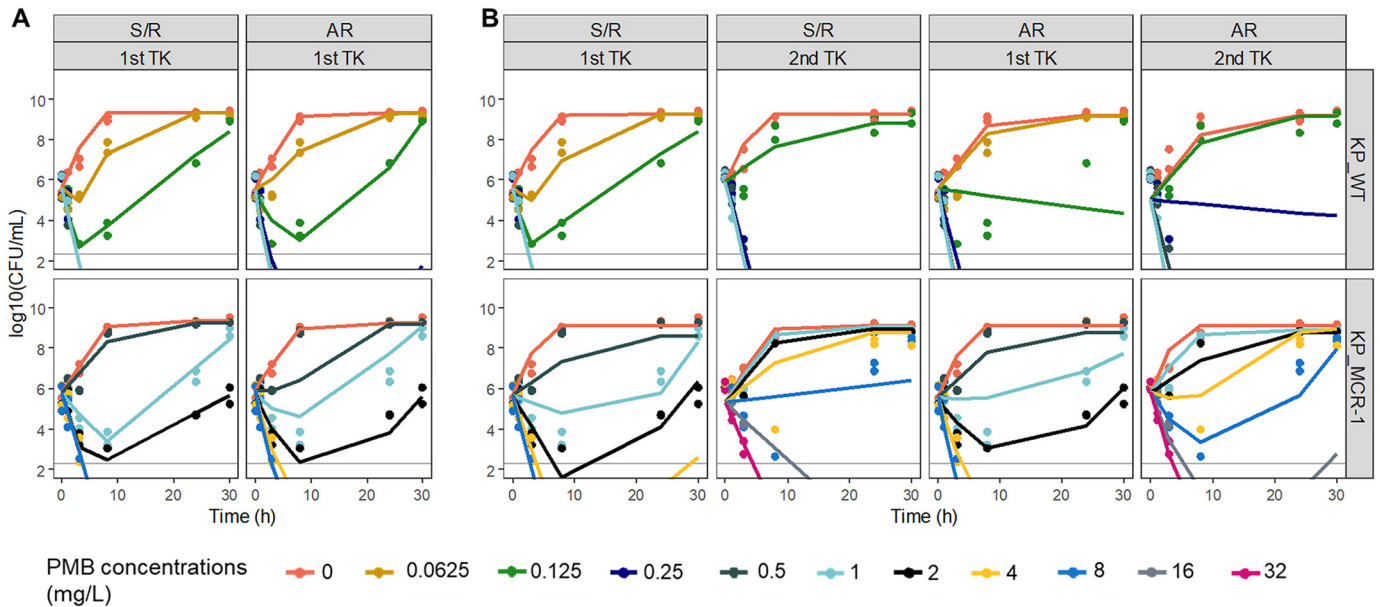


**FIG 2** Comparison of predictions from the S/R and AR models after analysis of a single TK experiment (A) or after simultaneous analysis of the sequential TK data (B) for 2 isogenic isolates. (Top) *K. pneumoniae* R2292 (KP\_WT); (bottom) its MCR-1 transconjugant (KP\_MCR-1). For KP\_WT, PMB concentrations ranging from 0.0625 to 1 mg/liter were used for the 2 sequential TK experiments. For KP\_MCR-1, PMB concentrations ranging from 0.5 to 8 and 1 to 32 mg/liter were used for the first and second TK experiments, respectively. Symbols, experimental data ( $n = 2$ ); color-matched lines, model predictions; gray solid lines, limit of quantification.

reduced, no initial CFU decay was observed at a concentration of 0.125 mg/liter anymore, but no regrowth was observed after the rapid decay observed at 0.25 mg/liter, consistent with (S) and (R) stable heterogeneous subpopulations (Fig. 2B, top). Accordingly, the S/R model was still able to describe the experimental data after simultaneous analysis of the two sequential TK experiments and to quantify the phenotypic difference between the two subpopulations with precision, with the reduced apparent activity for the (R) population reflected by an  $EC_{50,R}$  value ( $EC_{50,R}$ ) that was slightly higher than that for the (S) population ( $EC_{50,S}$ ) (0.132 versus 0.065 mg/liter). In contrast, with KP\_MCR-1, regrowth was observed at concentrations of 1 and 2 mg/liter after the first TK experiment and again after the second TK experiment, but at slightly higher concentrations of 4 and 8 mg/liter (Fig. 2B, bottom), indicating that PMB continued to lose efficacy during the second TK experiment. This sustained changing activity with time is not consistent with a stable (R) subpopulation but rather suggests continuous adaptation with time. Only the AR model was able to provide a relatively good fit of these sequential TK data for KP\_MCR-1.

However, these models were not really supported by RT-qPCR investigations. No mutation was observed with KP\_WT to support the two heterogeneous subpopulations for the S/R model. With KP\_MCR-1, an overexpression was observed for the *mcr-1* gene but with the same magnitude (5.5-fold) at the end of the first and second TK experiments compared with time zero, which is not consistent with continuous progressive adaptation during the first and second TK experiments. In this study, only two simple models, representative of the two basic situations, i.e., stable heterogeneous subpopulations (S/R) versus unstable homogenous population (AR), were tested. Although they provided relatively good fit, these models were not supported by the mechanistic experiments, suggesting that real life is likely to be more complex, with combined heterogeneity and instability issues requiring more complex models (1). Furthermore, mutant selection or adaptation phenomena may occur slowly and only be observable after several days of hollow-fiber experiments, which remain the most demanding but best approach for *in vitro* semimechanistic PK/PD modeling of antibiotics (10–12). Yet, although this study suffers from limitations, it shows that sequential TK experiments

**TABLE 1** Statistical comparison of various parameters for S/R and AR models

Parameter <sup>a</sup>	Model results [estimate and relative standard error <sup>b</sup> (%) for strain:							
	KP_WT				KP_MCR-1			
	1 TK		Sequential TK		1 TK		Sequential TK	
	S/R	AR	S/R	AR	S/R	AR	S/R	AR
BIC	23.4	39.5	35.1	208.8	14.1	47.1	163.7	86.5
INOC (log <sub>10</sub> CFU/ml)	5.60 (2.1)	5.52 (2.5)	5.63 (2.0)	5.55 (4.1)	5.78 (1.8)	5.9 (2.5)	5.64 (2.9)	5.56 (2.2)
INOC <sub>2</sub> (log <sub>10</sub> CFU/ml)			5.93 (0.9)	5.03 (3.2)			5.3 (2.6)	5.85 (1.9)
B <sub>max</sub> (log <sub>10</sub> CFU/ml)	9.29 (1.2)	9.32 (1.1)	9.24 (1.3)	9.19 (2.0)	9.34 (1.6)	9.24 (1.4)	9.1 (1.6)	9.13 (1.0)
mutf (log <sub>10</sub> CFU/ml)	-3.69 (9.0)		-3.49 (10.4)		-4.46 (8.9)		-10.5 (7.8)	
K <sub>g</sub> (h <sup>-1</sup> )	1.54 (8.1)	1.15 (15.2)	1.42 (10.4)	0.935 (20.1)	(S), 1.03 (12.8); (R), 0.568 (8.0) <sup>c</sup>	0.959 (15.9)	(S), 1.64 (20.0); (R), 1.19 (8.4) <sup>c</sup>	1.58 (7.9)
E <sub>max</sub> (h <sup>-1</sup> )	4.40 (5.9)		4.36 (4.8)		3.24 (6.4)		5.41 (10.3)	
E <sub>max(0)</sub> (h <sup>-1</sup> )		5.18 (8.2)		4.92 (13.7)		5.28 (10.8)		7.43 (7.0)
EC <sub>50</sub> (mg/liter)		0.121 (5.7)		0.371 (14.3)		1.85 (23.3)		6.98 (14.6)
EC <sub>50,S</sub> (mg/liter)	0.0631 (2.2)		0.065 (15.6)		0.932 (7.2)		1.87 (31.0)	
EC <sub>50,R</sub> (mg/liter)	0.141 (1.3)		0.162 (4.5)		3.9 (13.8)		31.1 (18.1)	
γ	10 (fixed) <sup>d</sup>	2.39 (15.1)	5.01 (15.3)	3.33 (33.4)	3.8 (18.7)	1 (fixed) <sup>e</sup>	1 (fixed) <sup>e</sup>	1 (fixed) <sup>e</sup>
K <sub>on</sub> (h <sup>-1</sup> )		0.0956 (17.5) <sup>f</sup>		0.001 (1.2) <sup>f</sup>		0.0856 (17.2) <sup>f</sup>		0.0547 (7.5) <sup>g</sup>
K <sub>on50</sub> (mg/liter)								2.89 (7.4)
δ								3.63 (9.8)
σ (log <sub>10</sub> CFU/ml)	0.255 (19.3)	0.382 (20.4)	0.29 (10.7)	1.97 (14.9)	0.226 (17.0)	0.498 (18.1)	0.825 (13.3)	0.469 (8.4)

<sup>a</sup>INOC, bacterial count at time 0 (before the start of the 1st TK); INOC<sub>2</sub>, bacterial count at 30 h (before the start of the 2nd TK); B<sub>max</sub>, maximum bacterial population size supported by the system; mutf, fraction of resistant bacteria (R) at time 0; K<sub>g</sub>, apparent growth rate constant; E<sub>max</sub>, maximum kill rate constant; E<sub>max(0)</sub>, maximum kill rate constant when no adaptive resistance has developed; EC<sub>50</sub>, PMB concentration that produces 50% of E<sub>max(0)</sub>; EC<sub>50,S</sub> and EC<sub>50,R</sub>, PMB concentrations that produce 50% of E<sub>max</sub> for the (S) and (R) subpopulations, respectively; γ, Hill coefficient in PMB effect relationship; K<sub>on</sub>, rate constant for development of adaptive resistance to PMB; K<sub>on50</sub>, PMB concentration yielding 50% of K<sub>on</sub>; δ, Hill coefficient for rate constant for development of AR; σ, additive residual error on log<sub>10</sub> scale for total bacteria count.

<sup>b</sup>Relative standard error obtained by sampling importance resampling.

<sup>c</sup>The sensitive (S) and resistant (R) subpopulations were assumed to grow at different rates, with the estimation of 2 different K<sub>g</sub> for (S) and (R) resulting in a significant decrease in the objective function value given by NONMEM.

<sup>d</sup>The Hill coefficient for this relationship, initially estimated to fall between 10 and 20, was fixed to 10 to improve model stability (13).

<sup>e</sup>PMB bactericidal effect was modeled using an ordinary E<sub>max</sub> model, with the estimation of Hill coefficient resulting in a nonsignificant decrease in the objective function value given by NONMEM.

<sup>f</sup>K<sub>on</sub> was estimated in the presence of PMB but was not dependent on its concentration.

<sup>g</sup>The resistance onset rate was determined by the PMB concentration through a sigmoid E<sub>max</sub> model. K<sub>on</sub> corresponds to the maximal rate constant for development of AR in this case.

constitute a simple approach to disqualify S/R models selected after traditional TK experiments and that these S/R models should not be used without further validation to predict treatment outcomes after multiple dosing.

**ACKNOWLEDGMENTS**

This work was funded by INSERM U1070 Laboratory, Université de Poitiers, and an LPDP scholarship (Indonesia Endowment Fund for Education).

**REFERENCES**

- Nielsen EI, Friberg LE. 2013. Pharmacokinetic-pharmacodynamic modeling of antibacterial drugs. *Pharmacol Rev* 65:1053–1090. <https://doi.org/10.1124/pr.111.005769>.
- Jacobs M, Grégoire N, Couet W, Bulitta JB. 2016. Distinguishing antimicrobial models with different resistance mechanisms via population pharmacodynamic modeling. *PLoS Comput Biol* 12:e1004782. <https://doi.org/10.1371/journal.pcbi.1004782>.
- Poirel L, Kieffer N, Brink A, Coetzer J, Jayol A, Nordmann P. 2016. Genetic features of MCR-1-producing colistin-resistant *Escherichia coli* isolates in South Africa. *Antimicrob Agents Chemother* 60:4394–4397. <https://doi.org/10.1128/AAC.00444-16>.
- Beal SL. 2001. Ways to fit a PK model with some data below the quantification limit. *J Pharmacokinet Pharmacodyn* 28:481–504. <https://doi.org/10.1023/A:1012299115260>.
- Jumbe N, Louie A, Leary R, Liu W, Deziel MR, Tam VH, Bachhawat R, Freeman C, Kahn JB, Bush K, Dudley MN, Miller MH, Drusano GL. 2003. Application of a mathematical model to prevent in vivo amplification of antibiotic-resistant bacterial populations during therapy. *J Clin Invest* 112:275–285. <https://doi.org/10.1172/JCI16814>.
- Campion JJ, McNamara PJ, Evans ME. 2005. Pharmacodynamic modeling of ciprofloxacin resistance in *Staphylococcus aureus*. *Antimicrob Agents Chemother* 49:209–219. <https://doi.org/10.1128/AAC.49.1.209-219.2005>.
- Meagher AK, Forrest A, Dalhoff A, Stass H, Schentag JJ. 2004. Novel pharmacokinetic-pharmacodynamic model for prediction of outcomes with an extended-release formulation of ciprofloxacin. *Antimicrob Agents Chemother* 48:2061–2068. <https://doi.org/10.1128/AAC.48.6.2061-2068.2004>.
- Mohamed AF, Nielsen EI, Cars O, Friberg LE. 2012. Pharmacokinetic-pharmacodynamic model for gentamicin and its adaptive resistance with predictions of dosing schedules in newborn infants. *Antimicrob Agents Chemother* 56:179–188. <https://doi.org/10.1128/AAC.00694-11>.
- Schmittgen TD, Livak KJ. 2008. Analyzing real-time PCR data by the comparative C(T) method. *Nat Protoc* 3:1101–1108. <https://doi.org/10.1038/nprot.2008.73>.
- Chung P, McNamara PJ, Campion JJ, Evans ME. 2006. Mechanism-based pharmacodynamic models of fluoroquinolone resistance in *Staphylococ-*

- cus aureus*. Antimicrob Agents Chemother 50:2957–2965. <https://doi.org/10.1128/AAC.00736-05>.
11. Tsuji BT, Bulitta JB, Brown T, Forrest A, Kelchlin PA, Holden PN, Peloquin CA, Skerlos L, Hanna D. 2012. Pharmacodynamics of early, high-dose linezolid against vancomycin-resistant enterococci with elevated MICs and pre-existing genetic mutations. J Antimicrob Chemother 67: 2182–2190. <https://doi.org/10.1093/jac/dks201>.
  12. Landersdorfer CB, Rees VE, Yadav R, Rogers KE, Kim TH, Bergen PJ, Cheah S-E, Boyce JD, Peleg AY, Oliver A, Shin BS, Nation RL, Bulitta JB. 2018. Optimization of a meropenem-tobramycin combination dosage regimen against hypermutable and nonhypermutable *Pseudomonas aeruginosa* via mechanism-based modeling and the hollow-fiber infection model. Antimicrob Agents Chemother 62:e02055-17. <https://doi.org/10.1128/AAC.02055-17>.
  13. Bulitta JB, Yang JC, Yohann L, Ly NS, Brown SV, D'Hondt RE, Jusko WJ, Forrest A, Tsuji BT. 2010. Attenuation of colistin bactericidal activity by high inoculum of *Pseudomonas aeruginosa* characterized by a new mechanism-based population pharmacodynamic model. Antimicrob Agents Chemother 54:2051–2062. <https://doi.org/10.1128/AAC.00881-09>.